Surface Reconstruction of the Unstable {110} Surface in Gold Nanorods

Z. L. Wang,*,† R. P. Gao,† B. Nikoobakht,‡ and M. A. El-Sayed*,‡

Electron Microscopy Center, School of Materials Science and Engineering, Georgia Institute of Technology, Atlanta, Georgia 30332-0245, and Laser Dynamics Laboratory, School of Chemistry and Biochemistry, Georgia Institute of Technology, Atlanta, Georgia 30332-0400

Received: March 1, 2000; In Final Form: April 22, 2000

Gold nanorods prepared electrochemically and capped in micelles are examined using high-resolution transmission electron microscopy (TEM). It is found that they have an axial growth direction of [001] and have surfaces made of {100} and the unstable {110} facets. A detailed examination of the defect sites of both of these facets shows that while the defective regions of the stable {100} facets show atom-height steps with no reconstruction, the less stable higher energy {110} surfaces show missing-row reconstruction. The role of micelles in stabilizing the {110} facet in the gold nanorod is briefly discussed.

Semiconductor nanoparticles or nanocrystals have been studied extensively recently because of their new properties[1−3] acquired on account of the reduction in their sizes. Metallic nanoparticles have a great promise for many applications such as catalysis,[4] photocatalysis,[5] sensors,[6] opticals,[7] electronic,[7] and magnetic.[8] Besides quantum size effects, their large surface-to-volume ratio and the large difference in the properties of their surface atoms, new properties, such as effective trapping dynamics in semiconductor nanoparticles[1−3] and effective catalysis properties[4] for metallic nanoparticles, are expected for materials in this size domain. In addition, noble metals, such as gold, exhibit[9−12] strong absorption due to the surface plasmon oscillation of their conduction electrons in the visible region of the spectrum as their size is reduced. This leads to strong coupling with the electric field of light, thus enhancing many linear and nonlinear processes such as surface Raman scattering, enhanced fluorescence of gold nanorods,[13] and second harmonic generation.[14] Catalysis with transition metals is known to depend on the crystal facets. Nanoparticles have been synthesized with different shapes, and each shape is shown to have different facets.[16]

As a result of broken bonds, atoms on surfaces tend to locate at new positions that may be different from the sites determined by the symmetry of the crystal, thus, a new unit cell is defined to describe the surface structure. This atom rearrangement is known as surface reconstruction, and the most typical[17] example is the 7×7 reconstruction of Si{111}. Surface reconstruction has been extensively investigated for a large range of materials under a variety of experimental conditions, and this field is a branch of modern surface science.[18] Extensive research has been carried out on the reconstruction of {110} bulk surfaces of nobel metals, and extensive literature exists discussing the 1×2 reconstruction of the {110} type surface.[19−24] Surface reconstruction of nanocrystal surfaces, however, remains to be investigated as a function of shape or size, and it remains to examine the effect of capping in determining the structure of their surfaces.

Scanning tunneling microscopy[25] (STM) is a powerful approach for directly imaging surface reconstruction. The application of this technique to nanoparticles, particularly the shape-controlled particles, is constrained because the particle surfaces are usually encapsulated by a layer of long-chain polymer molecules, such as the case for Pt.[15] This prohibits direct imaging of surface atoms of the particles. Removing the capping polymer usually requires thermal treatment at a temperature of ~200 °C or higher,[26] which may significantly change the as-prepared surface configuration of the particles.

In the Pt nanoparticles, for example, the different shapes are found to have either the {100} facets in the cubic nanoparticles, the {111} facets in the tetrahedral nanoparticles, or a mixture of {100} and {111} in the truncated octahedral nanoparticles.[16] The {100} and {111} are low-energy surfaces and their formation is expected. These facets are also observed in the gold nanodot nanocrystals.[27,28] However, gold nanorods formed electrochemically and capped with micelles are found to have mostly the {100} and the relatively unstable {110} facets.[29]

In this letter, the surfaces of the as-prepared Au nanorods are studied, for the first time, using high-resolution transmission electron microscopy (HRTEM) to carefully examine and compare the structure of the defective regions on the stable {100} and the higher energy {110} facets. Only the latter showed reconstruction into more stable facets. A model is proposed to explain the formation of the reconstructed surfaces. Discussion is given regarding its formation.

Gold nanorods were prepared by an electrochemical method described by Yu et al.[26] The electrolyte consisted of a hydrophilic cationic surfactant, hexadecyltrimethylammonium bromide, and a hydrophobic cationic cosurfactant, tetradecylammonium bromide or tetraoctylammonium bromide. The electrolysis was carried out under ultrasonication with an applied current of 5 mA and at a temperature of 42 °C for about 45 min. The optical properties[30] and dynamic processes involved in the formation and growth of gold nanoclusters such as atomic gold diffusion on the carbon surface have been investigated by in-situ TEM.[31] For the study reported here, a droplet of solution containing the Au nanorods was dispersed on ultrathin carbon film supported by copper meshes. After drying in air, the Au nanorods were studied at 400 kV using a JEOL 4000EX high-resolution TEM.

The surfaces of the Au nanorodes are fairly rough when observed at the atomic-scale resolution. Previous study[29] has revealed that the gold nanorods were confined by the {100}

* Corresponding authors.
† School of Materials Science and Engineering.
‡ School of Chemistry and Biochemistry.

10.1021/jp000800w CCC: $19.00
Published on Web 05/16/2000

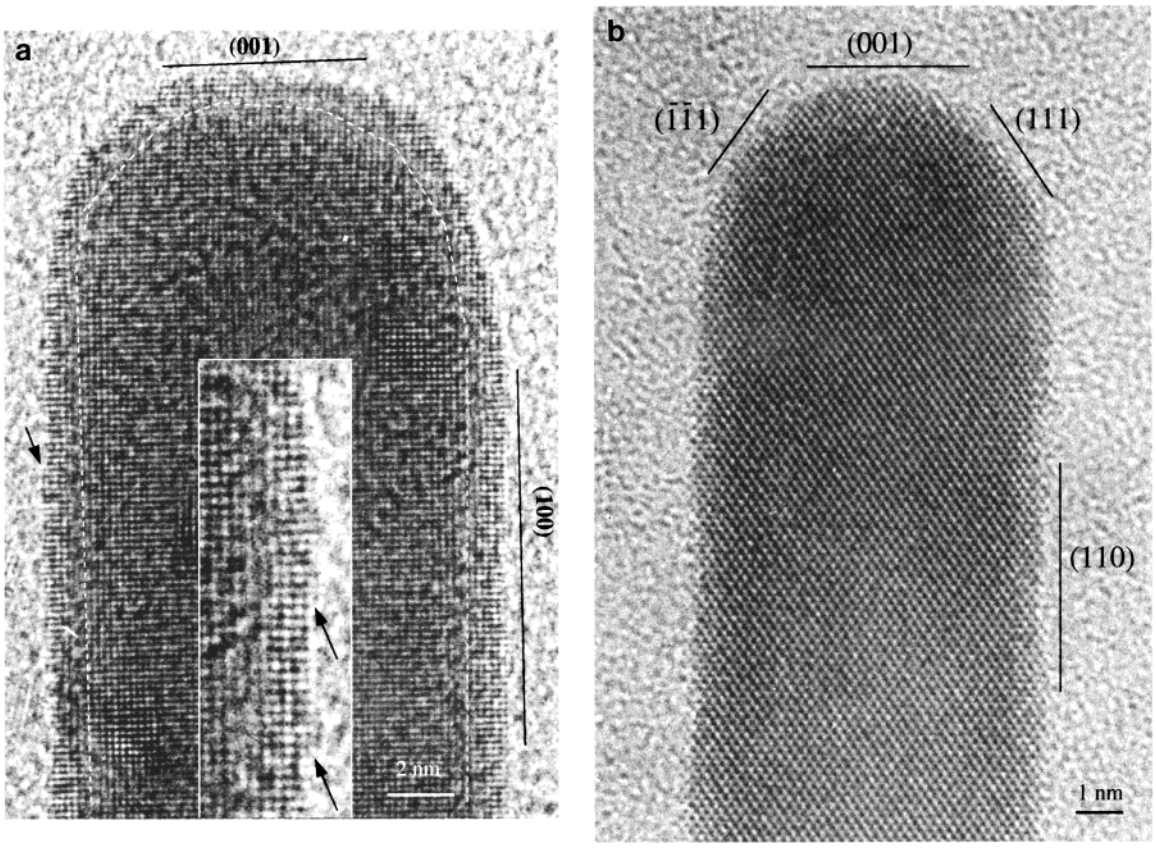

Figure 1. (a) High-resolution TEM image of the as-prepared Au nanorods oriented along (a) [010] and (b) [1 $\bar{1}$ 0]. The facets of the Au nanorods were imaged in profile. These images shows the distribution of the atoms on the (100) and (110) surfaces, respectively, as viewed in profile in parallel to the surface. The surface steps and surface reconstructions can be directly captured from the images.

and {110} faces and the growth direction was [001]. The presence of the {110} facets is a unique feature of Au nanorods and is not commonly observed because the {110} facet has higher energy than that of the {111} and {100} facets.[32] It would thus be interesting to compare the displacement of atoms at point defects on the different surfaces of gold nanorods.

Figure 1a shows a high-resolution TEM image of an Au nanorod oriented with its [010] parallel to the incident electron beam. In this case, the (001) and the (100) faces are images edge-on. An enlargement of the (100) surface is inset, which clearly shows the presence of atom-height surface steps, as indicated by the arrows, but the surface atoms show no reconstruction. Another interesting phenomenon observed in the image is the presence of a contour following the curvature of the nanorod, as schematically marked by a white dashed line, along which the contrast of the image is minimum. The image contrast is minimum at a specific thickness due to the vanishing intensity of the diffracted beams, such as (200), due to dynamic scattering.[33] The formation of this contour indicates the change in projected thickness across the Au nanorod, corresponding to the presence of the {110} type of facets. Figure 1b gives a high-resolution TEM image of a Au rod oriented along [1$\bar{1}$0]. The (110), (001), (111) and ($\bar{1}$ $\bar{1}$ 1) surface are imaged edge-on. The most interesting feature in this image is that the rows of surface atoms are imaged clearly so that we can analyze the configuration of the rearrangement.

Figure 2 shows the enlarged surface profile images of the (110) surface of the Au nanorod and the corresponding models representing the rows of atoms arranged near the surface. Although the amorphous substrate reduces the image contrast, the atom distribution near the surface is still resolvable. In some regions, rows of atoms are missing along [1 $\bar{1}$ 0] and the surface

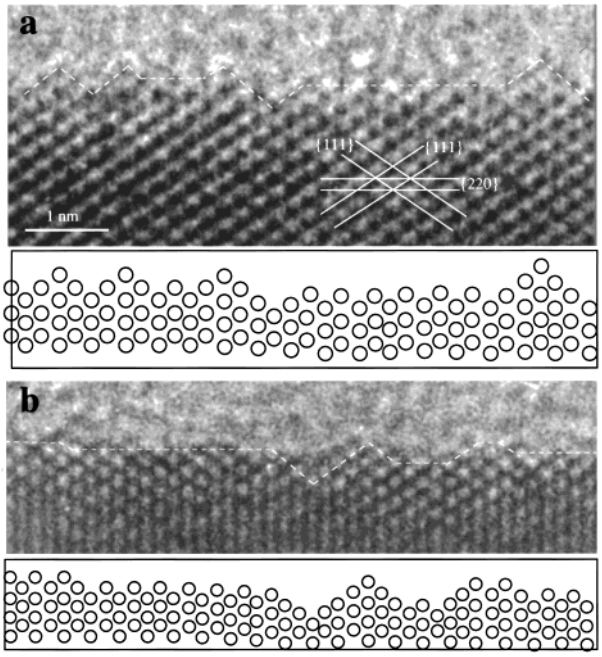

Figure 2. High-resolution TEM images recorded from an Au nanorod oriented along [110] and the corresponding positions of the projected atom rows, showing the rearrangement of the surface atoms.

can be qualitatively described to be an irregular "saw-tooth" structure. If the rows of missing atoms are perpendicular to the direction of the incident electron beam, the image would show the perfect (110) surface for the face-centered cubic (fcc) lattice. Figure 3 gives high-resolution TEM images of the (110) surface. The missing rows are observed fairly frequently. In the areas

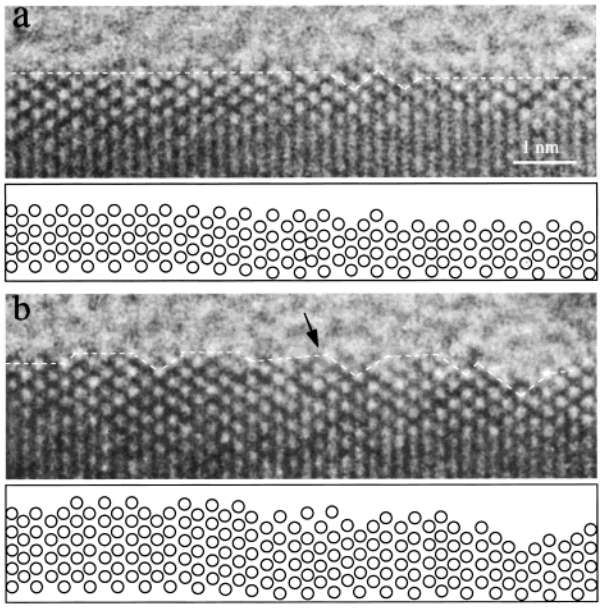

Figure 3. High-resolution TEM images recorded from an Au nanorod oriented along [110] and the corresponding positions of the projected atom rows.

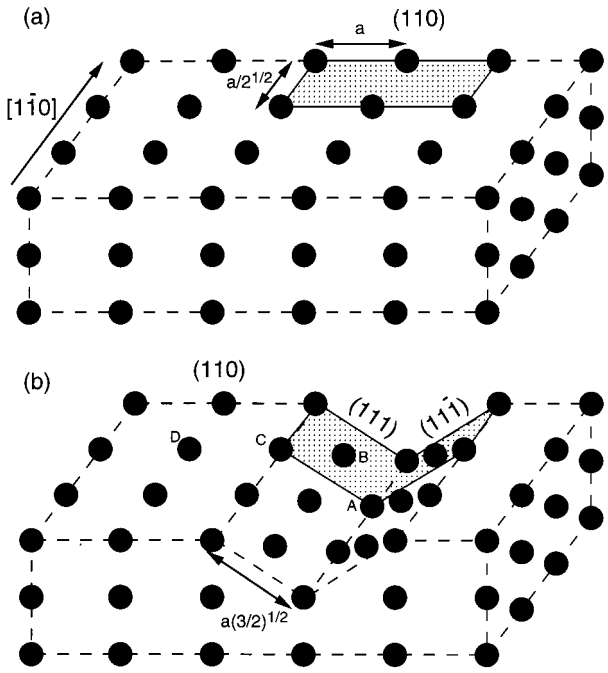

Figure 4. Atomic models of (a) an ideal (110) surface and (b) the reconstructed (110) surface with missing rows. A unit cell (pasted in gray) is defined for the calculations of the broken bonds in the text.

such as the one indicated by the arrow in Figure 3b, the atomic columns deviate significantly from the lattice sites determined by symmetry, which result from the relaxation of surface atoms.

To understand the surface reconstruction, Figure 4a shows a schematic model for the perfect (110) surface built from the fcc lattice. If a row of atoms is missing along [1 $\bar{1}$ 0], the (110) surface transforms into strips of {111} facets. It is known that the {111} surface is the most densily packed surface for fcc structure and is thus the most stable surface. We take the unit cell as marked in Figure 4 as an example to illustrate the change in surface energy as a result of surface reconstruction. If we consider only the interaction between the first nearest neighbor of the Au atoms (separated by $a/2^{1/2}$, where a is the lattice constant of Au), the nearest neighbors lost by atoms A, B, C, and D marked in the figure after reconstruction are 1, 3, 5, and 5, respectively. The total nearest neighbors per unit cell lost by the atoms before and after reconstruction are 10 and 12, respectively, and the surface area changes from $2^{1/2}a^2$ to $3^{1/2}a^2$. If each nearest neighbor forms a chemical bond, the number of broken bonds per unit surface area for an ideal (110) surface is $7.071/a^2$, and is $6.928/a^2$ for the reconstructed surface. The total number of broken bonds per unit surface area decreases after the reconstruction. Therefore, the surface energy is lower after the reconstruction.

A major question is why was the {110} surface present. The surface of the Au nanorods was encapsulated by a micelle, which not only confines the geometry of the Au nanorod but also stabilizes the surface atoms of the {110} facets. The fact that the bonding between the surface gold atoms is not strong on the {110} facet, due to larger interatomic distance, allows each atom to form stronger bonds with adsorbed or bonded atoms on this surface. If the miscelles bind to the surface via the Br^- ions of the surfactants used, charge transfer to the gold atoms on the {110} surface would probably give stronger bonds than those formed solely between the gold atoms with their neighbors as on the {110} facets. The question is why do we see the reconstruction occurring on certain regions of the {110} facets of the nanorod? We believe that reconstruction occurs at defect sites where the capping micelle molecules are missing. Work is now planned in which the removal of the micelle and the extent of the reconstruction is examined as a function of the thermal annealing temperature. Hence, the number of the broken bonds may not change even after the surface is formed because the surface is tightly enclosed by the micelle molecules. On the other hand, the volume of Au nanorods is almost defect free, and defects tend to move toward the surface if they exist. Rearrangement of surface atoms may be necessary to accommodate the surface defects, including point defects.

From an energy point of view, the {110} surface observed is unlikely to be stable after removing the capping layer by heating to ~200 °C. Therefore, the surface atoms tend to diffuse at relatively low temperature, as observed previously.[31]

In conclusion, atom rearrangement on the surfaces of the as-prepared Au nanorods was investigated by high-resolution TEM. The {100} surface shows atom-height surface steps, and the {110} surface exhibits the missing-row reconstruction. It was suggested that the reconstruction of the {110} surface is stable because of the presence of the capping molecules.

Acknowledgment. The research was supported by NSF CHE-9727633 and NSF DMR-9733160. Thanks to the Georgia Tech Electron Microscopy Center for providing the experimental facility.

References and Notes

(1) For a review see: (a) Steigerwald, M. L.; Brus, L. E. *Acc. Chem. Res.* **1990**, *23*, 183. (b) Wang, Y.; Harron, N. *J. Phys. Chem.* **1991**, *95*, 525. (c) Wang, Y. In *Advances in Photochemistry*; Neckers, D. C., Ed.; John Wiley & Sons: New York, 1995; Vol. 19, p 179.

(2) (a) Haase, M.; Weller, H.; Henglein, A. *J. Phys. Chem.* **1988**, *92*, 4706. (b) Henglein, A. *Chem. Rev.* **1989**, *89*, 1861.

(3) (a) Rossetti, R.; Brus, L. E. *J. Phys. Chem.* **1986**, *90*, 558. (b) Chestnoy, N.; Harris, T. D.; Hull, R.; Brus, L. E. *J. Phys. Chem.* **1986**, *90*, 3393.

(4) Hirai, H.; Wakabayashi, H.; Komiyama, M. *Chem. Lett.* **1983**, 1047.

(5) Brugger, P.-A.; Cuendet, P.; Gratzel, M. *J. Am. Chem. Soc.* **1981**, *103*, 2923.

(6) Thomas, J. M. *Pure Appl. Chem.* **1988**, *60*, 1517.

(7) Charles, S. C.; Popplewell, J. In *Ferromagnetic Materials*; Wohlharth, E. P., Ed.; North-Holland: Amsterdam, 1980; Vol. 2.

(8) Clint, J. H.; et al. *Faraday Discuss. Chem. Soc.* **1993**, *95*, 219.

(9) Papavassiliou, G. C. *Prog. Solid State Chem.* **1980**, *12*, 185.
(10) Kerker, M. *The Scattering of Light and Other Electromagnetic Radiation*; Academic Press: New York, 1969.
(11) Bohren, C. F.; Huffman, D. R. *Absorption and Scattering of Light by Small Particles*; Wiley: New York, 1983.
(12) Kreibig, U.; Vollmer, M. *Optical Properties of Metal Clusters*; Springer: Berlin, 1995.
(13) Mohamed, M. B.; Volkov, V.; Link, S.; El-Sayed, M. A. *Chem. Phys. Lett*., in press.
(14) Boyd, G. T.; Yu, Z. H.; Shen, Y. R. *Phys. Rev. B* **1986**, *33*, 7923.
(15) Ahmedi, T.; Wang, Z. L.; Green, T. C.; El-Sayed, M. A. *Science* **1996**, *272*, 1924.
(16) Wang, Z. L.; Ahmedi, T.; El-Sayed, M. A. *Surf. Sci.* **1997**, *380*, 302.
(17) Takayanagi, K.; Tanishiro, Y.; Takahashi, S.; Takahashi, M. *Surf. Sci.* **1985**, *164*, 367.
(18) See, for example: Pick, S. *Surf. Sci. Rep.* **1991**, *12*, 99. Bernasconim, T. E. *Surf. Sci. Rep.* **1991**, *17*, 363.
(19) Rost, M. J.; van Gastel, R.; Frenken, J. W. M. *Phys. Rev. Lett.* **2000**, *84*, 1966.
(20) Li, S. Y.; Li, R. S.; Guan, R. N.; Ye, H. Q.; Zhu, J. *J. Electron Microsc.* **2000**, *49*, 163.
(21) Yamaghishi, T.; Takahashi, K.; Onzawa, T. *Surf. Sci.* **2000**, *445*, 18.
(22) Vilfan, I.; Lancon, F.; Adam, E. *Surf. Sci.* **1999**, *440*, 279.
(23) Lee, J. I.; Mannstadt, W.; Freeman, A. J. *Phys. Rev. B* **1999**, *59*, 1673.
(24) Koch, R.; Sturmat, M. *Surf. Sci.* **1998**, *404*, 861.
(25) See, for example: (a) Wiesenanger, R., Ed. *Scanning Tunneling Microscopy I: General Principles and Applications to Clean and Adsorbate-Covered Surfaces;* Springer Series in Surface Sciences; Springer: New York 1994; (b) Bai, C. *Scanning Tunneling Microscoopy and Its Application*; Springer Series in Surface Sciences; No. 32, Springer: New York 1995.
(26) Yu, Y.-Y.; Chang, S.-S.; Lee, C.-L.; Wang, C. R. *J. Phys. Chem. B* **1997**, *101*, 666.
(27) Flueli, M.; Spycher, R.; Stadelmann, P. A.; Buffat, P. A.; Borel, J.-P. *Europhys. Lett.* **1988**, *6*, 349.
(28) Marks, L. D. *Rep. Prog. Phys.* **1994**, *57*, 603.
(29) Wang, Z. L.; Mohamed, M. B.; Link, S.; El-Sayed, M. A. *Surf. Sci*. **1999**, *440*, L809.
(30) Link, S.; Burda, C.; Mohamed, M. B.; El-Sayed, M. A. *J. Phys. Chem. B* **1998**, *103*, 11.
(31) Mohamed, M. B.; Wang, Z. L.; El-Sayed, M. A. *J. Phys. Chem. A* **1999**, *103*, 10255.
(32) Hakkinen, H.; Merikoskii, J.; Manninen, M. *J. Phys.: Condens. Matter* **1991**, *3*, 2755.
(33) Wang, Z. L.; Kang, Z. C. *Functional and Smart Materials − Structural Evolution and Structure Analysis*; Plenum: New York, 1998; Chapter 6.